

Semianalytical Modeling of Concrete Beams Rehabilitated with Externally Prestressed Composites

Abhijit Mukherjee¹; Shivprasad P. Bagadi²; and Gopal L. Rai³

Abstract: This study attempts to develop a semianalytical model for the mechanical behavior of reinforced concrete (RC) beams rehabilitated with externally prestressed carbon fiber-reinforced polymers (CFRP) laminates. The main significance of this study is the model of the process of degradation of RC beams until failure and its recovery through externally prestressed CFRP. Experiments have been carried out to observe the load–deflection behavior of fresh RC beams until the load resistance of the beam is exhausted. The beams have been rehabilitated with external CFRP laminates with varying levels of prestress. The rehabilitated beams have been reloaded until failure. The load–deflection behavior of the fresh and rehabilitated beams has been compared. A model for the load–deflection behavior of the fresh and rehabilitated beam has been proposed. The main import of the model is that it incorporates the effect of confinement of concrete. The model shows very good agreement with the experimental results.

DOI: 10.1061/(ASCE)1090-0268(2009)13:2(74)

CE Database subject headings: Concrete beams; Laminates; Prestressing; Cross sections; Rehabilitation.

Introduction

Reinforced concrete, although a very popular construction material, suffers from aging and deterioration. Demolition and rebuilding of aged structures may not be feasible due to financial, spatial, sentimental, logistic, and technical constraints. Restoration can be an attractive alternative if the issues of uncertain performance due to unproven techniques, materials, and design methods could be addressed. Recent development in the carbon fiber-reinforced polymer (CFRP) in rehabilitation of structures is being seriously investigated by the researchers as a sound and cost effective technique. Alternatively in practice, CFRPs are just beginning to get a toehold in the construction industry, especially in the upgradation of existing structures.

FRPs improve confinement of concrete and thus enhance its capacity in compression (Mukherjee et al. 2004). FRPs have also been effective in augmenting the reinforcement in bending members (Ramana et al. 2000). The seismic performance of reinforced concrete (RC) frame structures can also be dramatically improved by externally bonding FRP at the beam–column joints (Mukherjee and Joshi 2005). A spin-off from FRP wraps is protection of steel in concrete (Gadve et al. 2009). The resistance to corrosion and higher specific strength make these materials ideal for externally reinforcing existing structures with minimum intrusion. The popular method adopted in such cases is adhesively bonding FRPs on concrete structures. However, the superior strength of

FRPs can seldom be fully utilized due to poor capacities of the concrete and the interfaces.

Prior research on modeling of prestressed FRPs includes load–deflection relationships for concrete beams reinforced either by steel or glass FRP bars (Alsayed 1998); serviceability of flexural FRP reinforced concrete members (Aiello and Ombres 2000); studies on externally bonded laminates (Arduini and Nanni 1997; EI-Mihilmy and Tedesco 2000); and nonlinear analysis of reinforced concrete beams strengthened with externally bonded FRP laminates (Kwak and Kim 2002; Kim and Lee 1992). There are some instances of the use of external bonding technology in rehabilitating deteriorated structures. However, a theoretical model for the prediction of performance of the structure is unreported. In the present study, a systematic method for the mechanical model of deteriorated RC beams that are rehabilitated with externally prestressed laminates is attempted. The model has been validated with experiments.

Experimental Work

The experimental process has been described in Mukherjee and Rai (2009). In this paper essentials for the analytical work are included. Properties of the materials used in the experimentation are enlisted in this section.

Concrete

Concrete mix was prepared using Portland cement blended with fly ash. Properties of cement and concrete are shown in Tables 1 and 2, respectively.

Steel Reinforcement

Longitudinal reinforcement of beams is high yield strength deformed steel bars and shear links are of mild steel. Properties of reinforcing steel are in Table 3.

¹Director, Thapar Univ., Patiala—147 006, India.

²Graduate Student, Dept. of Civil Engineering, Indian Institute of Technology Bombay, Mumbai—400 076, India.

³Graduate Student, Dept. of Civil Engineering, Indian Institute of Technology Bombay, Mumbai—400 076, India.

Note. Discussion open until September 1, 2009. Separate discussions must be submitted for individual papers. The manuscript for this paper was submitted for review and possible publication on October 12, 2006; approved on September 26, 2008. This paper is part of the *Journal of Composites for Construction*, Vol. 13, No. 2, April 1, 2009. ©ASCE, ISSN 1090-0268/2009/2-74–81/\$25.00.

Table 1. Physical Properties of Cement

Physical properties	Value
Fineness (m^2/kg)	374
Setting time (min)	
• Initial setting time	180
• Final setting time	270
Compressive strength (MPa)	
• 3 days	33
• 7 days	44
• 28 days	56
Percentage of fly ash in cement	24

FRP Materials

Composite materials used for the study are commercially available worldwide. Two types of CFRPs, sheets and laminates, have been used (Fig. 1). The laminates have been prestressed and used in the longitudinal direction of the beams. The sheets have been used in the ends to protect the edges. Table 4 details the test results of the CFRP materials and Table 5 contains the details of the adhesive.

Adhesives

The adhesive used for all the experiments is a compatible epoxy system recommended by the manufacturer. It has two components, A=resin and B=hardener. The ratio of the components by weight is 100 parts of Component A to 23 parts of Component B. Mixing is done thoroughly for 5 min with a low speed mixer at 400 revolutions/min until components are thoroughly dispersed. Properties of adhesive are given in Table 6.

Specimen Preparation

Beams of length 1.8 m and cross section 90 mm wide and 180 mm deep are used. Detailed dimensions and reinforcements are shown in given Fig. 2.

Flexure Tests

Four-point flexure tests have been carried out on the control beams first. The beams were loaded until they stopped offering any resistance to the load. The beams were rehabilitated using prestressed FRP and then they were subjected to the same load regime.

Table 2. Properties of Concrete

Physical properties	Value
28 days compressive strength (MPa)	32
Modulus of elasticity (GPa)	21.22
Slump (mm)	56

Table 3. Properties of Steel Reinforcement

Reinforcement type	Modulus of elasticity (E_s) (GPa)	Characteristic strength (F_y) (MPa)
Longitudinal tor bars	200	515
Mild steel shear links	200	250

**Fig. 1.** CFRP materials used in the experiment

Fresh Beam Tests

All RC beam specimens have been loaded in a four-point bend test setup as shown in Fig. 3. This test has been carried out on the RC beams prior to the application of any FRP. The setup ensures pure bending in the central third portion of the beam. They have been loaded with equal force on the two load points until the beams did not take any further load. A deflection controlled experiment was carried out and the load rate was kept slow at 0.5 mm/s. The deflection of the beam was monitored with linear variable differential transducers. It may be noted that the beam sections were underreinforced, therefore, steel had yielded in all the specimens. The damage in the beams started with bending cracks in the central region of the beam. At higher load levels the shear and shear-bending cracks at the end sections had initiated. At higher levels of deformation the cracks coalesced with a rapid

Table 4. Properties of CFRP Laminate

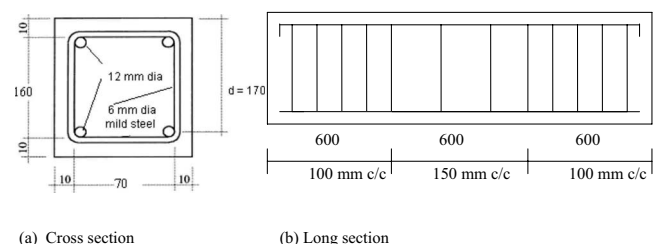
Properties	Test results
Width	50.8 mm
Thickness	1.4 mm
Ultimate tensile strength	2.51 GPa
Percentage elongation at break	1.8
Tensile modulus	155 GPa

Table 5. Properties of CFRP Sheet

Properties	Test results
Mass per square meter	644 g/m ²
Ultimate tensile strength	876 MPa
Tensile modulus	72.46 GPa
Percentage elongation at break	1.2

Table 6. Properties of Epoxy

Items	Test results
Tensile strength	21.4 MPa
Tensile strain failure	5%
Flexural modulus	1,690 MPa
Flexural strength	40.7 MPa
Glass transition temperature	80°C

**Fig. 2.** Details of beam specimens

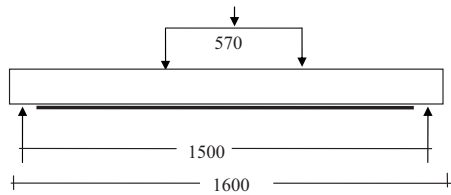


Fig. 3. Four-point bend setup

loss of stiffness. The loading was discontinued when the load-deflection curve was flat and no increase load was observed due to the increase in deflection. After unloading the permanent deformations have been recorded. Load deflections were similar for all the samples.

Prestressing

The prestressing was undertaken using a specially designed machine (Fig. 4). The ends of the laminate were attached to the drums; but the laminate was kept slack. The adhesive was uniformly spread on the top surface of the laminate, as well as on the bottom surface of the beam. The beam was placed on the laminate. The ends of the beam were secured with the drums by means of anchors. This was necessary because the specimens had already bent in the first phase of test. The movable drum was rotated by a self-locking screw jack system to give required tension to the laminate. There was marginal recovery of the permanent deformation of the beams due to the upward thrust produced by the prestressed laminate on the bent beam. The laminate had a strain gauge at its center to record the longitudinal strain. The force was measured by correlating load versus strain curve for the CFRP, as well as by a load cell fixed to the prestressing machine. In all prestressed beams CFRP sheets were used to avoid peeling of the laminate from the ends. The adhesive was allowed to cure for 5 days. The prestressing force was slowly released by turning the screw jack. Thus, the beam experienced and recovered some of the permanent deformation. The loss of prestress was monitored for a period of three days. The rehabilitated beams were finally tested for flexure. CFRP laminate to nonprestressed beams was also applied on the prestressing machine, but the force in the laminate was maintained as 50 N to keep it taut.

Test Results

The load-central deflection curves of the beam at all the different phases of test have been plotted in Fig. 5. The fresh beams have been loaded until their load resistance was exhausted; then the

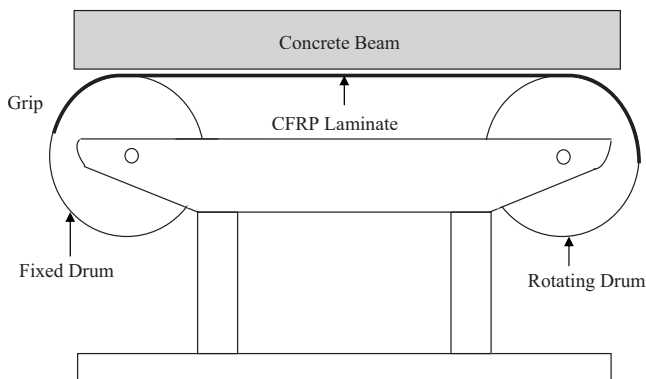


Fig. 4. Prestressing machine

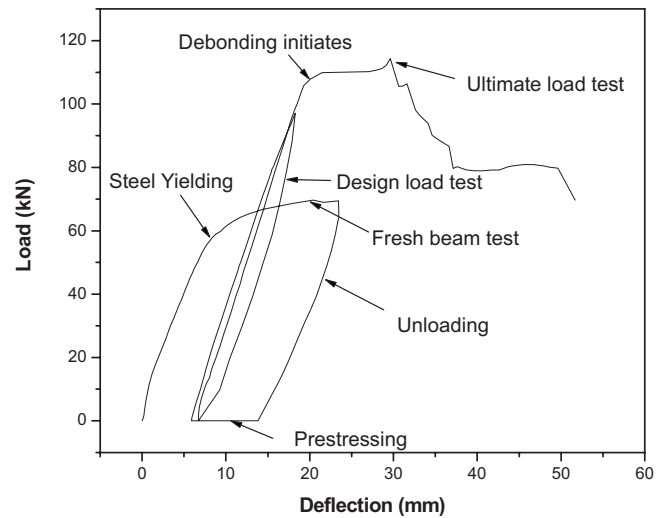


Fig. 5. Load-deflection curve for RC beams

beams were unloaded. The permanent deformation was measured. The beam was rehabilitated. The rehabilitation includes prestressing. The rehabilitated beams have been loaded up to the design load and unloaded. The permanent deformation in the beam is measured once again. The beams have been loaded once again until failure.

A detailed account of the test procedure is included elsewhere (Mukherjee and Rai 2009). Here we shall focus on the semianalytical model and validation.

Theoretical Model

The theoretical model has been developed in different scales. The response of a structure under load depends, to a large extent, on the stress-strain relation of the constituent materials. It has thus been necessary to define the constitutive relationships of all the materials. The material scale model has been used on the cross section of the element to obtain a cross-section scale model. This model is in the form of moment-curvature relations for the cross section. Utilizing the cross-section model the element model has been developed to predict the load-deflection relation of the beam. The element model can be used in determining the overall behavior of the structure that consists of several elements.

Material Scale Model

Concrete

As concrete is used mostly to withstand compression, the stress-strain relation in compression is of primary interest. The initial modulus of elasticity (E_0) of concrete is determined by concrete cylinder tests. The failure stress is determined through cube tests to maintain compatibility with Indian Code IS456 (Bureau of Indian Standards 2000). We shall briefly discuss the different models that have been considered.

IS Code Model

IS456 suggests a standard constitutive model for concrete. The constitutive behavior of concrete in compression is assumed to be

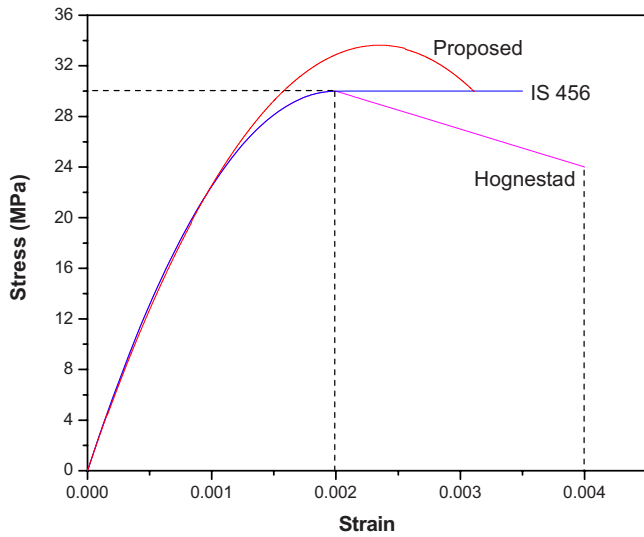


Fig. 6. Stress–strain curve for concrete as per IS 456, proposed model and Hognestad model

parabolic up to strain 0.002 and then it follows a straight horizontal line up to failure (Fig. 6). It ignores the degradation of concrete at strains beyond 0.002. Thus the constitutive relation is expressed as

$$\sigma_c = \left[\frac{2\varepsilon}{\varepsilon_0} - \left(\frac{\varepsilon}{\varepsilon_0} \right)^2 \right] f_{ck} \quad \text{for } 0 < \varepsilon < 0.002$$

$$\sigma_c = f_{ck} \quad \text{for } 0.002 < \varepsilon < 0.004 \quad (1)$$

where σ_c = stress in concrete at any point of strain; ε = strain at any point; ε_0 = strain at which parabolic part ends = 0.002; and f_{ck} = characteristic compressive strength of concrete.

Hognestad Model

The Hognestad model includes the damage parameter of concrete. The stress–strain curve before maximum stress reached is a parabola and then the falling branch behavior is adopted depending on the limit of useful strain (Fig. 6)

$$\sigma_c = \begin{cases} \left[\frac{2\varepsilon}{\varepsilon_0} - \left(\frac{\varepsilon}{\varepsilon_0} \right)^2 \right] f_{ck} & \text{for } 0 < \varepsilon < 0.002 \\ [1 - 100(\varepsilon - \varepsilon_0)] f_{ck} & \text{for } 0.002 < \varepsilon < 0.004 \end{cases} \quad (2)$$

One shortcoming of the model is that it ignores the level of confinement provided by the lateral reinforcement. The useful strain in concrete depends on the confinement of concrete. This may not be very important in the case of standard steel bar reinforced beams as the level of confinement is low; but for the externally wrapped beams this is a very important factor. It has been observed experimentally that the limiting longitudinal strain can be extended dramatically through external confinement. Therefore, the present work requires a new model of concrete that includes confinement.

Proposed Model

The present model is based on prior work (Mukherjee et al. 2004) on concrete columns with wrapped FRP. The model for uniform compression has been adopted in the present context for bending compression. The basic premise of the model is that the constitu-

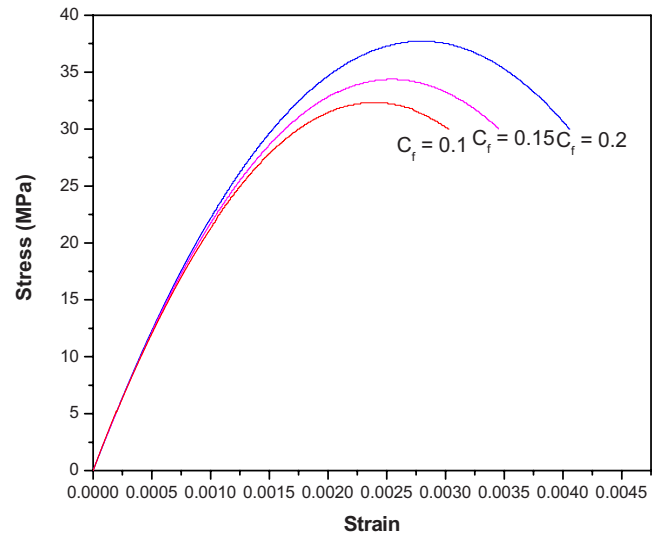


Fig. 7. Stress–strain relationship with varying confinement

tive behavior of concrete at low strains (before the initiation of damage) is governed by its initial modulus (E_0). However, the limiting strain (ε_{lim}) is determined by the level of confinement and the maximum stress is determined by its grade (f_{ck}). Therefore, the constitutive model is a function of all these parameters

$$\sigma_z = E(E_0, f_{ck}, \varepsilon_{lim}) \varepsilon \quad (3)$$

Fig. 6 shows the stress–strain curve for confined concrete. The stiffness of concrete decreases with the increase in axial compression. The rate of softening is largely influenced by the presence of lateral confinement. Fig. 7 shows the variation of stress–strain relationships with different degrees of confinement. The rate depends on the relative stiffness of the confining material and the concrete core. The limiting strain is considered as the function of confinement. The variable secant modulus (E) and limiting strain (ε_{lim}) is defined as follows:

$$E = \left(1 - \frac{\varepsilon}{\varepsilon_{lim}} \right) E_0 + \frac{\varepsilon f_{ck}}{\varepsilon_{lim}^2} \quad (4)$$

$$\varepsilon_{lim} = 0.002(1 + 5C_f) \quad (5)$$

where C_f = confinement is the confinement factor

This factor is a function of the relative stiffness of the confining material and the concrete core. The confinement factor is expressed as follows:

$$C_f = \left(\frac{E_f t_f + E_s t_s}{E_0 r} \right)^{0.5} \quad (6)$$

where C_f = confinement factor; E_f = modulus of elasticity of FRP; t_f = thickness of fiber; E_s = modulus of elasticity of steel; t_s = thickness of steel; E_0 = initial modulus of concrete; and r = effective radius. The present model has been compared with the existing models in Fig. 6. It is noted that the model matches very well at lower levels of strain. At higher strains the model shows higher ultimate maximum stress, but lower ultimate strain. It may be recalled that the model incorporates the effect of confinement. Therefore, it is important to examine the stress–strain curves for a range of confinements (Fig. 7). The confinement is defined in terms of confinement factor (C_f). As the confinement factor increases both the maximum stress and strain go up. The predicted curves are very similar to the test results (Mukherjee et al. 2004).

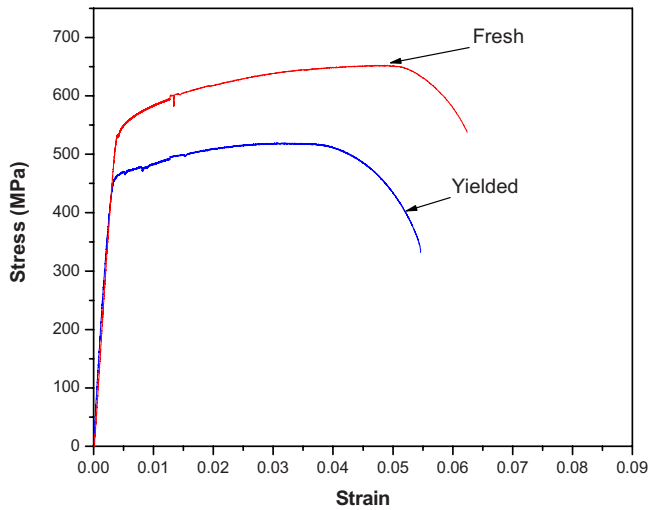


Fig. 8. Stress-strain relationship for steel

Steel

The stress-strain relationship for steel reinforcements is determined through experiments (Fig. 8). Two sets of reinforcements have been used—fresh and yielded bars after beam tests. The yielded bars were collected by digging them out of the beams after the tests. The yielded bar properties have been used in the rehabilitation phase of the calculation.

FRP Laminate

The FRP plates do not have any yield point like the steel reinforcement and are typically linear elastic up to rupture as shown in Fig. 9. The FRP plate material is assumed to be linear until rupture.

Cross-Sectional Scale Model

The material models are now scaled up to determine the property of the composite cross section. The classical moment-curvature relations of RC sections are developed.

Assumptions: To determine the moment capacity of the tension plated RC beam, the following assumptions are made:

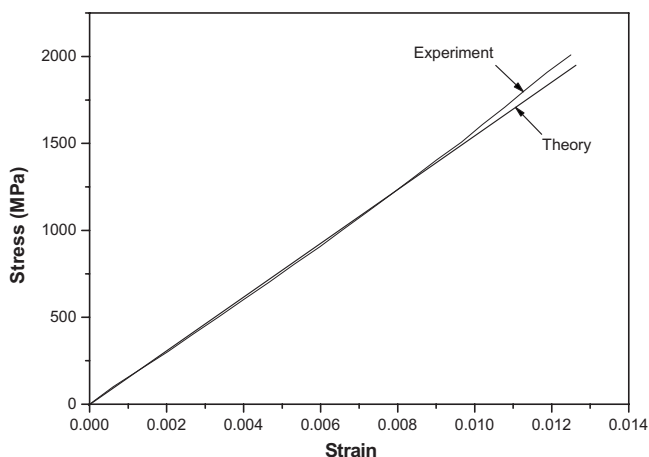


Fig. 9. Stress-strain relationship for CFRP plate

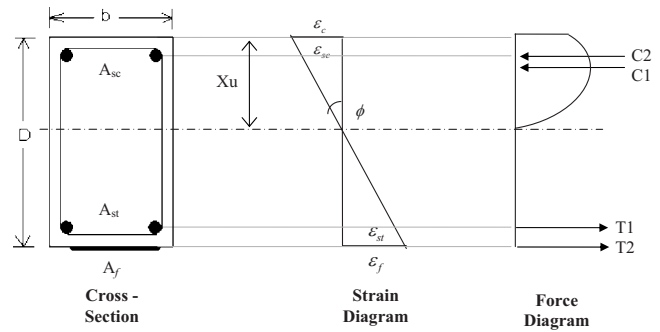


Fig. 10. Stress-strain distribution across the cross section

- Euler-Bernoulli hypothesis is considered, i.e., shear deformations are neglected;
- Concrete under tension is neglected;
- Perfect bonding between all the materials up to debonding of composites;
- Displacements are small; and
- Properties of steel in tension and compression are identical.

Based on the previous assumptions for a given curvature, the corresponding magnitude of the strain in the compression concrete (ε_c), compression steel (ε_{sc}), tension steel (ε_{st}), and strain in plate (ε_f) can be determined from the strain compatibility conditions. Fig. 10 shows the stress-strain distribution across the section. Further, the analytical procedure described is based on the above-mentioned assumptions. Fig. 10 shows the stress and strain distributions

$$\varepsilon_c = \phi X_u$$

$$\varepsilon_{sc} = \phi(X_u - d_c)$$

$$\varepsilon_{st} = \phi(d - X_u)$$

$$\varepsilon_f = \phi(D - X_u) \quad (7)$$

where ε_c =concrete compressive strain at the extreme compression fiber; ε_{sc} =strain in compression steel; ε_{st} =strain in tension steel; ε_f =strain in plate; ϕ =curvature given to the cross section; X_u =depth of neutral axis from compression face; d_c =effective cover to the compression steel; d =depth of centroid of tension steel; b, D =overall width and depth of the cross section; A_{sc}, A_{st}, A_f =area of compression steel reinforcement, tensile steel reinforcement, and FRP plate, respectively.

The equilibrium relation for the cross section can be written as

$$C = \sigma_{sc}A_{sc} + b \int_0^{X_u} \sigma_c dx$$

$$T = \sigma_{st}A_{st} + \sigma_f A_f$$

$$C = T \quad (8)$$

The equations have been solved numerically for X_u by iterations. The corresponding bending moment for a curvature can thus be calculated

$$M_c = b \int_0^{X_u} \sigma_c x dx$$

$$M_{sc} = \sigma_{sc}A_{sc}(X_u - d_c)$$

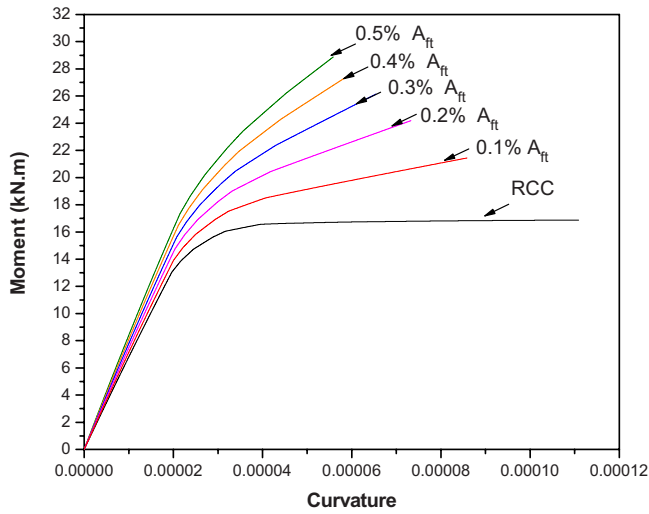


Fig. 11. Moment curvature relationship of RC beam

$$M_{st} = \sigma_{st} A_{st} (d - X_u)$$

$$M_p = \sigma_f A_f (D - X_u) \quad (9)$$

The bending moment at a section corresponding to the applied curvature is obtained from

$$M = M_c + M_{sc} + M_{st} + M_p \quad (10)$$

The moment–curvature relationship obtained for different levels of longitudinal reinforcement is presented in Fig. 11. In case of RC beams, failure is characterized by yielding with a large branch of plastic deformation. FRP strengthened beams show marginal change in initial stiffness. A substantial difference in the postyield behavior of the beam is noticed. With the increase in the FRP reinforcement the postyield stiffness increases monotonically. Thus, at a given curvature, the resisting moment of the beam would increase with increase in FRP. However, the maximum curvature also reduces with the increase in FRP. As a result, the beam resists higher bending moments but fails at a lower curvature. A trade-off between these two phenomena is necessary in the design. The failure of the FRP reinforced beams was due to compression failure of concrete. It may be noted that the failure strain of concrete can be improved [Eq. (7)] through increase in confinement. The confinement can be increased by wrapping FRP around the beam.

Element Scale Model

The moment–curvature relation obtained from the cross-section model is scaled up to determine the load–deflection behavior of the beam element. The solution has been obtained in incremental form

$$\Delta P_i = [k_i] \Delta \delta_i \quad (11)$$

where ΔP_i = incremental load in i th step; $\Delta \delta_i$ = incremental displacement in the i th step; and k_i = stiffness coefficient that is dependent on the slope of the moment–curvature relation at i th step.

The total loads and displacements are determined through the addition of the increments

$$P_i = \sum \Delta P_i$$

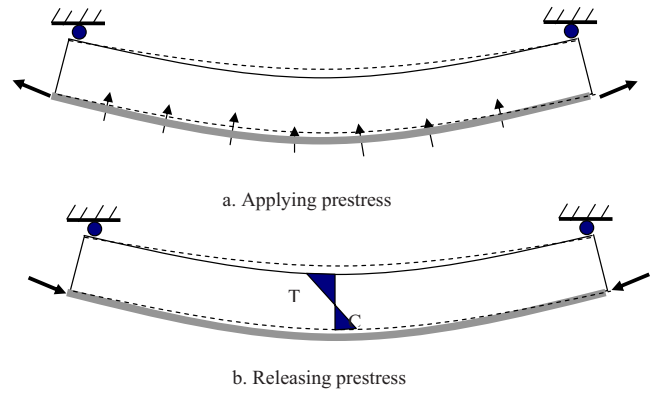


Fig. 12. Recovery due to prestressing

$$\delta_i = \sum \Delta \delta_i \quad (12)$$

However, there are several phases in the test procedure:

- Fresh beam loading;
- Unloading;
- Prestressing; and
- Reloading.

The element scale models for all these stages have been discussed here.

Fresh Beam Loading

In the loading phase the displacement of the beam is increased incrementally and the corresponding increment in the load is calculated. The stiffness coefficient for the four-point loading system is

$$K_i = \frac{a(3l^2 - 4a^2)}{24(EI)_i} \quad (13)$$

where l = distance between two supports of the beam and a = distance of point load from support. The method is iterative as the moment–curvature relation is nonlinear.

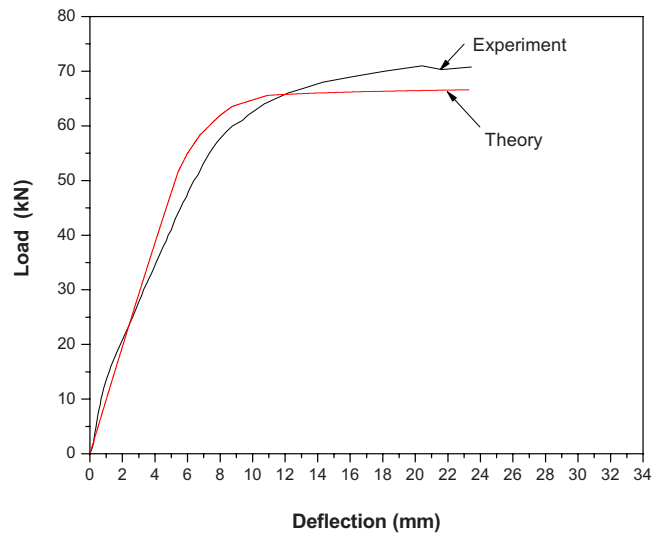


Fig. 13. Theoretical and experimental load–deflection curve of RC beam

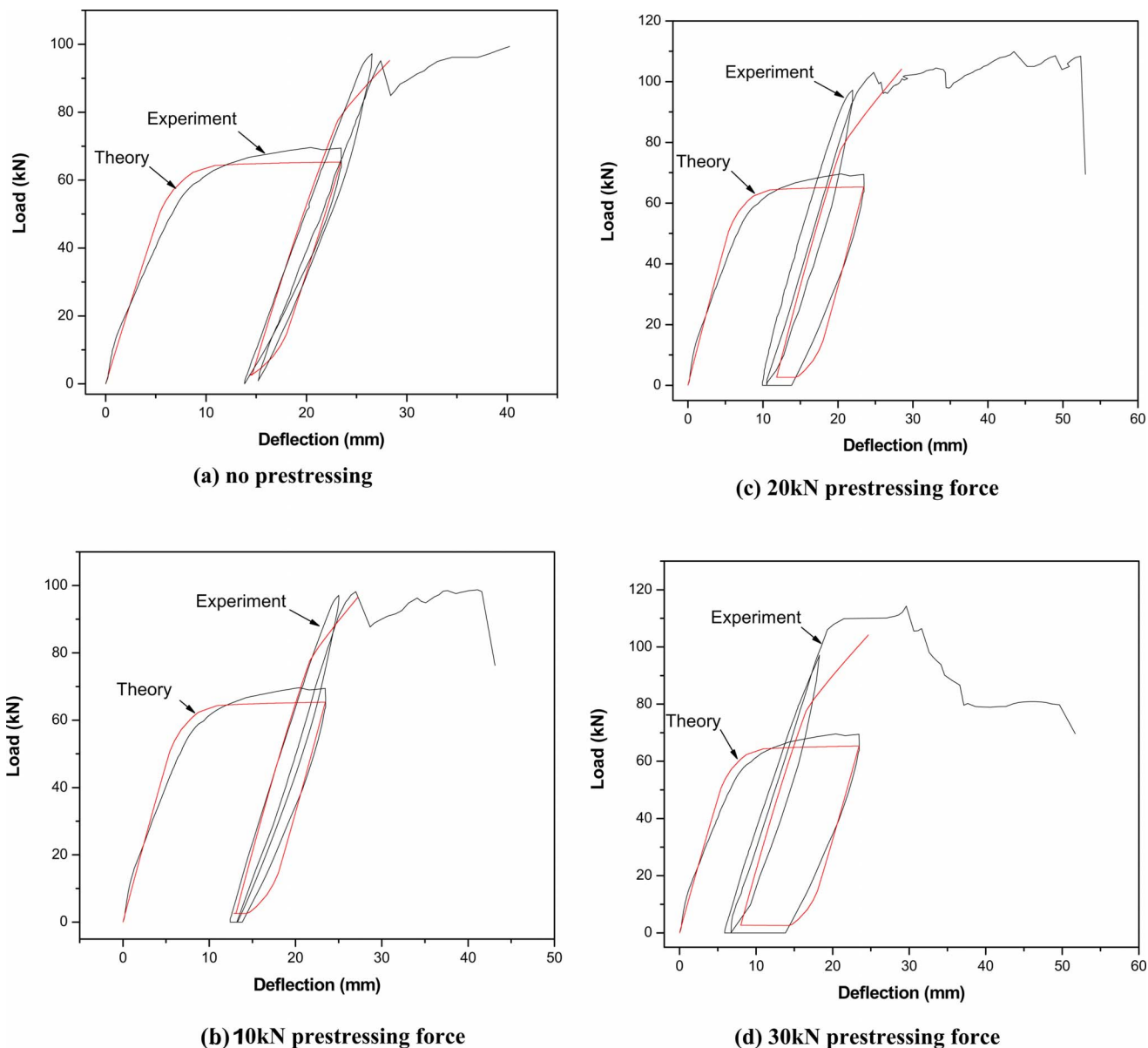


Fig. 14. Theoretical and experimental load–deflection curves with various levels of prestressing force

Unloading

The unloading model is essentially the same as the loading model with negative incremental displacement. In the present model a mirror image of the loading curve has been used in the unloading curve. It may be noted that the beam does not recover from the entire deformation, i.e., the beam remains curved even after the load has been totally withdrawn. This is the residual deformation in the beam.

Prestressing

During prestressing the beam recovers from its residual deformation. There are two stages of recovery—during the application of prestress on the laminate and during the release of the load from the machine. It may be noted that the ends of the beam are secured prior to the application of the prestress. The tension in the laminate applies a thrust on the beam that tends to straighten it [Fig. 12(a)]. The beam had another round of recovery when the prestress force was released from the machine [Fig. 12(b)]. This is

the classical recovery of the beam due to prestressing. Both these recoveries have been recorded and compared with the semianalytical model.

At the time of applying prestress

$$p = P/r \quad (14)$$

where r =radius of curved beam; p =Stress applied at the periphery of the beam; and P =Prestressing force. Upward deflection, due to moment, is determined by the elasticity concept and equal to upward deflection, due to moment, is determined by the elasticity concept and equal to

$$Ml^2/(8EI) \quad (15)$$

where EI =cracked flexural stiffness of the beam; M =end moment= $p \cdot e$, and l =length of the beam.

Reloading

In the reloading stage the theoretical model is same as that in the fresh beam. The additional contribution of the CFRP laminate is considered at this stage.

Results Validation

In this section, experimental results have been utilized to compare theoretical load–deflection diagrams with the experimentally observed ones. Fig. 13 shows the load–deflection diagrams of the fresh beam. It can be seen that the initial stiffness of the experimental curve is higher. However, the beam loses that stiffness at a fairly low level of loading and the two curves come very close. The contribution of concrete in tension is neglected in the theoretical model. Therefore, the experimental beam shows higher initial stiffness. The curves deviate from linearity through the yielding of steel in tension. Finally, the strain limit of steel is exceeded and that is considered as the failure point. The correlation between the two curves is very good. The postyield hardening behavior of the beam observed in the experiment is not reflected in the numerically obtained plot because the strain hardening is not considered in the theoretical model for steel.

The theoretical and experimental predictions of the entire loading cycle for different levels of prestressing are presented in Fig. 14. It may be noted that the theory and the experiment agree very well at all stages of loading. The unloading has been predicted very well and the residual deformation is in good agreement. The recovery due to all levels of prestress has been predicted accurately by the model. The theoretical values of the stiffness and the final load level of the rehabilitated beam had an excellent agreement with experiment. The deformation at the final stage of loading is due to the debonding of the laminate from the beam. This is not predicted by the theory as debonding is not included in the present model.

Concluding Remarks

This paper discusses an investigation on the mechanical behavior of deteriorated RC beams that have been rehabilitated with prestressed CFRP laminates. Experiments have been conducted to inflict damage in standard RC beams. The damaged beams have been rehabilitated using prestressed CFRP laminates. The level of prestress force has been varied to observe the extent of recovery of the beams.

A multiscale model for the prediction of mechanical behavior of rehabilitated RC beams has been presented. At the material scale the stress–strain behavior of all the ingredients has been developed. The model for concrete includes the effect of confinement by both steel rebars and externally wrapped FRP sheets. The cross-section scale model utilizes the material model to predict

the moment–curvature relations of the cross section. This model has been used in the development of the load–deflection behavior of the beam element. The model predicts the behavior of the beam at all stages of the experiment—loading, unloading, prestressing, and reloading. Very good agreement between the experimental results and the theoretical model has been observed. Although the present model predicts the ultimate load very accurately it does not predict the ultimate deflection. The deflection of the beam after the ultimate load is reached is governed by debonding. A debond model is under development and shall be reported in the future.

Acknowledgments

The present work is financially supported by the Board of Research in Nuclear Sciences, India and Department of Science and Technology, India. The writers also thank Fyfe India and Sika AG for donating the composite material system.

References

- Aiello, M. A., and Ombres, L. (2000). “Load–deflection analysis of FRP reinforced concrete flexural members.” *J. Compos. Constr.*, 4(4), 164–171.
- Alsayed, S. H. (1998). “Flexural behaviour of concrete beams reinforced with GFRP bars.” *Cem. Concr. Compos.*, 20(1), 1–11.
- Arduini, M., and Nanni, A. (1997). “Behavior of precracked RC beams strengthened with carbon FRP sheets.” *J. Compos. Constr.*, 1(2), 63–70.
- Bureau of Indian Standards. (2000). *Plain and reinforced concrete—Code of practice, IS 456*, 3rd Revision, New Delhi, India.
- El-Mihilmy, M. T., and Tedesco, J. W. (2000). “Analysis of reinforced concrete beams strengthened with FRP laminates.” *J. Struct. Eng.*, 126(6), 684–691.
- Gadve, S., Mukherjee, A., and Malhotra, S. N. (2009). “Corrosion of steel reinforcements embedded in FRP wrapped concrete, construction and building materials.” *Constr. Build. Mater.*, 23(1), 153–161.
- Kim, J. K., and Lee, T. G. (1992). “Nonlinear analysis of reinforced beams with softening concrete.” *Comput. Struct.*, 44(3), 567–573.
- Kwak, H. G., and Kim, S. P. (2002). “Nonlinear analysis of RC beams based on moment–curvature relation.” *Comput. Struct.*, 80(7–8), 615–628.
- Mukherjee, A., Bakis, C. E., Boothby, T. E., Maitra, S. R., and Joshi, M. V. (2004). “Mechanical behavior of FRP wrapped concrete—complicating effects.” *J. Compos. Constr.*, 8(2), 97–103.
- Mukherjee, A., and Joshi, M. (2005). “FRPC reinforced concrete beam–column joints under cyclic excitation.” *Compos. Struct.*, 70(2), 185–199.
- Mukherjee, A., and Rai, G. L. (2009). “Performance of reinforced concrete beams externally prestressed with fiber composites, construction and building materials.” *Constr. Build. Mater.*, 23(2), 822–826.
- Ramana, V. P. V., Kant, T., Morton, S. E., Dutta, P. K., Mukherjee, A., and Desai, Y. M. (2000). “Behavior of CFRPC strengthened reinforced concrete beams with varying degrees of strengthening.” *Composites, Part B*, 31(6–7), 461–470.